Indonesian Geotechnical Journal, December 2025, Vol 4 (3). Page 143-154
DOI: https://doi.org/10.56144/igj.v4i3.133
EISSN: 2829-7520
https://indonesian-geotechnical-journal.org/index.php/JGI/issue/archive

# Influence of Underconsolidating Soil on Effective Stress Path in a Deep Excavation Case

**Albert Sebastian[1] , Aswin Lim[2,*]**
[1]Department of Civil Engineering, Universitas Katolik Parahyangan, Bandung, Indonesia, 40141; 8102501017@student.unpar.ac.id
[2]Department of Civil Engineering, Universitas Katolik Parahyangan, Bandung, Indonesia, 40141; aswinlim@unpar.ac.id
*Correspondence: aswinlim@unpar.ac.id

**SUBMITTED** 18 November 2025 **REVISED** 15 December 2025 **ACCEPTED** 28 December 2025

**ABSTRACT** This study investigates the influence and impact of clay soil that is presumed to be undergoing consolidation process on an unbraced shallow excavation system. The excavation geometry spans up to 160 meters with a maximum depth of 5.25 meters. A concrete sheet pile wall was installed at the front side of the excavation, supported by additional tie beams connected to square precast piles behind the wall. Based on soil investigation data, residual excess pore water pressures were identified within the underconsolidating clay layer at depths between 3 to 12 meters. These residual pore pressures contribute additional loading to the retaining wall system. A back analysis was conducted to obtain appropriate soil parameters to be used for PLAXIS 2D modelling. The finite element analysis results were compared with inclinometer data to validate the back analysis. Modeling of the underconsolidating condition was performed by manually inputting the pore water pressure into the initial condition. Results show that under underconsolidating conditions, the maximum wall deflection reached 190 mm, whereas under hydrostatic conditions, it was only 100 mm. Additionally, a parametric study was carried out to examine the relationship between the degree of consolidation and wall deflection. The findings indicate that a higher degree of consolidation leads to reduced wall deflection. To investigate the stress changes on the wall due to underconsolidating soil, a stress path analysis was performed to understand the stress history around the excavation. It was found that in underconsolidating conditions, the average effective stress tends to be lower and the deviatoric stress higher, resulting in a stress path that is closer to the failure line.

**KEYWORDS** Back Analysis; Excavation; FEM; Stress Path; Underconsolidating

## 1 INTRODUCTION

Deep excavations are increasingly in demand in developing urban areas to accommodate transportation, utility, and building infrastructure. However, excavations in soft clay are challenging due to their low shear strength, high compressibility, and time-dependent consolidation behavior (Ou, 2021)

In reclamation areas such as North Jakarta, soft clays often remain in an underconsolidated state due to the additional loads imposed by fill materials used for reclamation (Setionegoro, 2013). According to Rahardjo (2008) the main problem of underconsolidating soils is the pore water pressure that remains trapped within the soft clay layer which can be detected from the piezocone test (CPTu). This underconsolidating condition may result in increased lateral pressure against retaining walls, inducing larger wall deformation. Conventional design assumptions that consider hydrostatic pore pressure distributions may therefore underestimate the true magnitude of wall movement and ground settlement in such environments (Lim et al., 2016).

To evaluate soil behavior under different loading conditions and possible soil responses, it is essential to examine the stress path (Budhu, 2011). Several studies have demonstrated the critical role of soil stress paths especially in excavation cases. For example, Becker (2011) numerical study of stress path in soft soil excavation emphasized that stress paths must be taken into account to understand soil behavior through its stress history to obtain realistic simulation of construction process. Similarly, Lim et al. (2017) investigated stress path trends under undrained conditions and

highlighted their influence on deformation predictions. While these studies highlight the importance of stress path considerations, few have explicitly examined stress path behavior in underconsolidating conditions especially in deep excavation cases.

This study mainly investigates the influence of underconsolidating soil conditions on deep excavation behavior in North Jakarta by evaluating the wall deflections and the surface settlements. The research was conducted using finite element analyses with MC (Mohr-Coulomb) and HS (Hardening Soil) models. Back analyses were conducted by comparing numerical predictions with inclinometer data to validate the model. In addition, a parametric study is carried out by varying the degree of consolidation to assess the effect of pore pressure dissipation on wall deflections and settlements. Most importantly, stress path analyses were performed to interpret the soil stress–strain responses under excavation loading, with comparisons between hydrostatic and underconsolidating conditions and between MC and HS models to evaluate performance of each constitutive models in capturing stress path direction.

## 2 METHODS

### 2.1 Case Description

The excavation project is located at reclaimed land of North Jakarta, Indonesia. The excavation was constructed for the requirement of a one level basement for 24 stories office building. Figure 1a and 1b shows the location and plan view of the excavation project.

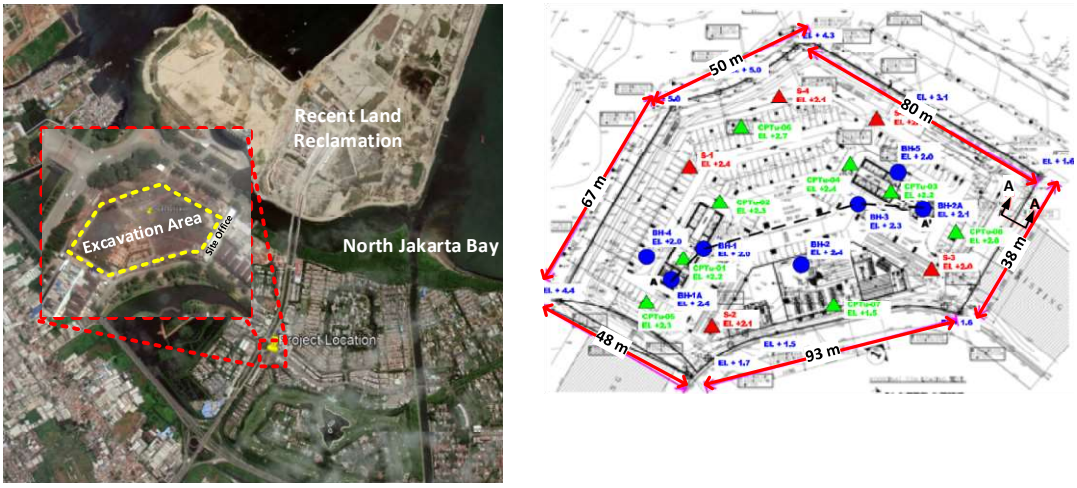


(a) (b)

Figure 1. (a). Project location and (b). plan view of the excavation

The excavation was designed in a diamond shaped layout, with a maximum span of approximately 93 m and a depth of 5.25 m. The retaining system primarily consists of corrugated concrete sheet pile (CCSP) walls, which were tied back using reinforced concrete beams. These beams functioned to transfer the lateral loads to the rear support system, which comprised of square precast concrete piles.

### 2.2 Soil Stratification

In general, the soil strata of North Jakarta excavation are divided into 7 layer according to field investigations. The artificial sandy silt fill is 3 m thick. Followed by the underconsolidating soil layer of very soft to soft clay which is 9 m thick. Next layer is a 6 m thick stiff clay followed by a layer of dense sand of 5 m thick. Underneath the sand layer, a thick stiff clay layer of 17 m was found. The last 2 layers are a thick stiff clay layer of 20 m each with the lower layer exhibiting a higher degree of consistency compared to the overlying one. Figure 2 shows the soil stratification of the project.

### 2.3 Finite Element Modelling

Two dimensional (2D) finite element analysis was conducted using PLAXIS 2D software. **Figure 2** shows the finite element mesh used to conduct the analysis. Plane strain type analysis was conducted for this case, therefore only half of the excavation geometry was modeled. Fifteen-node triangular elements were used simulate the soil cluster with fine mesh. To minimize the influence of boundary effects, the model was extended vertically to a depth of 80 m and horizontally to 40 m behind the retaining wall, thereby allowing reliable simulation of ground deformation and settlement behavior behind the wall.

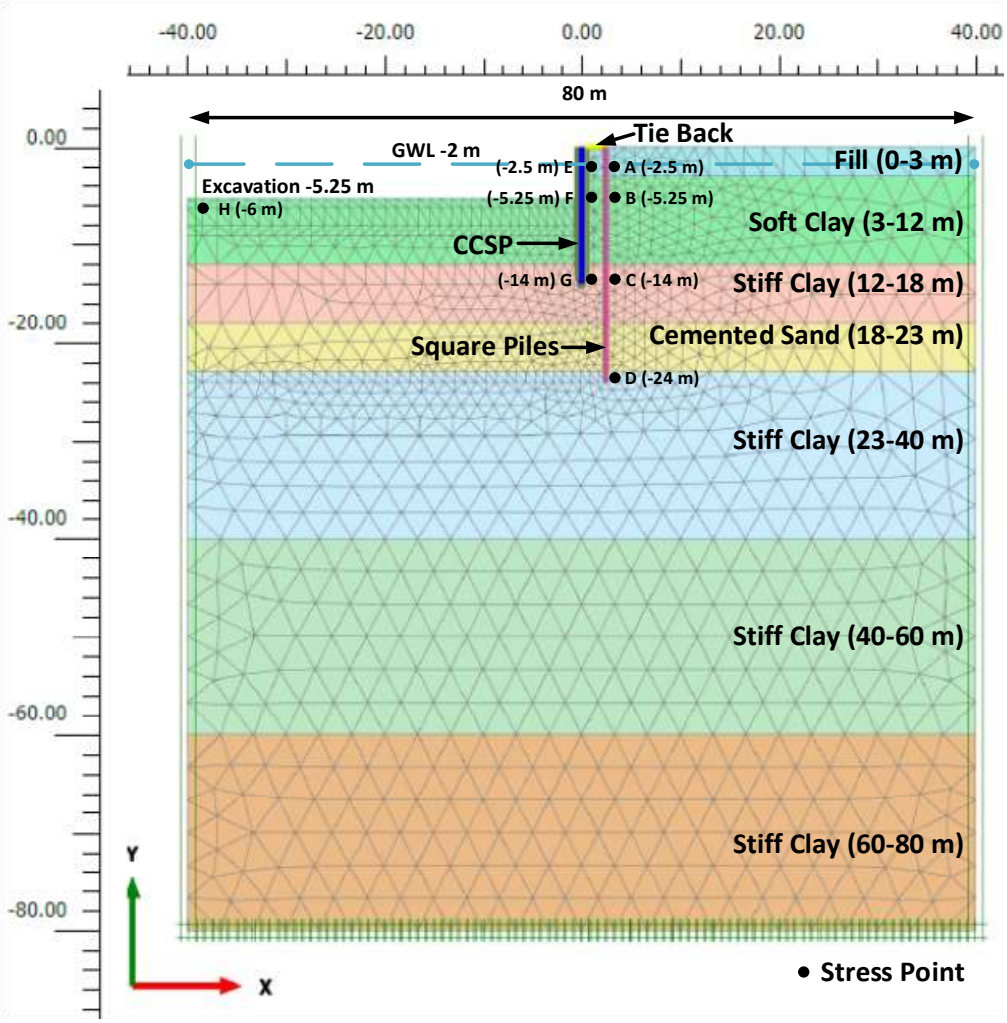


Figure 2 Finite element model and geometry for analysis

#### 2.3.1 Soil and Structure Model

The analyses were conducted in both Mohr–Coulomb (MC) and Hardening Soil (HS) constitutive models. An effective stress approach was adopted, in which fine-grained soils were modeled using the Undrained A, while coarse-grained soils were modeled as Drained. Preliminary soil parameters were derived from $N_{SPT}$ correlation and supplemented with data from a previous study in the same area (Lim et al., 2016). The unit weight ($\gamma_t$) values were selected based on the correlation proposed by Lambe et al (1962). Modulus of elasticity was estimated by using soil consistency correlation provided by Look (2007). Shear strength parameters of c' and $\phi$' were determined with reference to AS 4678-2002.

For HS model, additional parameters were required to conduct analysis including modulus of unloading-reloading ($E_{ur}^{ref}$) and modulus of oedometer ($E_{oed}^{ref}$). These parameters were calculated using equation proposed by Calvello and Finno (2004) where $E_{50}^{ref} = 3\ E_{ur}^{ref}$ and $E_{oed}^{ref} = 0.7\ E_{50}^{ref}$. The conversion from $E_{ur}$ to $E_{ur}^{ref}$ was performed using Equation (1) as proposed by Schanz et al (1999).

$$E_{ur} = E_{ur}^{ref}\left(\frac{c\cos\varphi - \sigma'_3 \sin\varphi}{c\cos\varphi + p_{ref}\sin\varphi}\right)^m \quad (1)$$

The soil parameters are back-analyzed until the deformation from the analysis best-matched to the one obtained from field measurements. The soil parameters are discussed in the next section.

Three structural elements were modeled. The parameters for corrugated concrete sheet piles, the tie back beam and square piles are shown in Table 1. All structural elements were assumed to behave linear-elastic. The modulus of elasticity ($E$) was determined using the equation $E = 4700\sqrt{f_c'}$, based on the concrete compressive strength. The cross-sectional area ($A$) represents the surface area of each element, while ($I$) denotes the moment of inertia. The Poisson's ratio of concrete was assumed to be 0.15. The unit weight ($w$) of each structural element, relative to the surrounding soil, was calculated using $w = (\gamma_{concrete} - \gamma_{soil}) \times A$. To compensate the occurrence of crack in concrete due to the large bending moment, the stiffness of all structural elements were reduced by 20% from the nominal value (Ou, 2021).

Table 1. Structural parameters input

| Type | Model | $E$ [kPa] | $A$ [m$^2$] | $I$ [m$^4$] | $\upsilon$ | $w$ [kN/m] |
|---|---|---|---|---|---|---|
| Square Piles | Embedded Beam | 18800000 | 0.25 | 0.001694 | 0.15 | - |
| Tie Beam | Plate | 18800000 | 1 | 0.083 | 0.15 | 6 |
| CCSP W-350A | Plate | 3903003.158 | 0.1468 | 0.005208 | 0.15 | 1.1744 |

To model underconsolidating conditions using 2D finite element analysis software, several methods can be employed to simulate underconsolidating conditions. In this study, two modeling approaches were implemented to generate pore water pressure within the soil. The first method, used for the back analysis, involved a user-defined approach in which excess pore water pressure values were manually assigned to the underconsolidating soil layer (soft clay). The second method, used for parametric study, the development of pore water pressure was simulated through consolidation analysis, where the addition of a fill layer in the model induced excess pore pressure within the soft clay layer.

### 2.3.2 Stage Construction

The construction phase for numerical modeling in general consisted of two scenarios. First is the initial condition of normally consolidated soil (hydrostatic condition). The second is initial condition of underconsolidating soil. Table 2 lists the modelling procedure for all scenarios where the initial condition was calculated using $K_0$ procedure and the conditions of hydrostatic or underconsolidating pore pressure will be manually inputted in initial condition.

Table 2. Modelled construction phase

| Phase | Staged Construction | Calculation Type | Pore Pressure |
|---|---|---|---|
| Initial Phase | Initial | $K_0$ Procedure | Phreatic |
| Phase 1 | Structural Element Activation | Plastic | Phreatic |
| Phase 2 | Excavation to -5.25 m | Plastic | Phreatic |

### 2.4 Stress Path

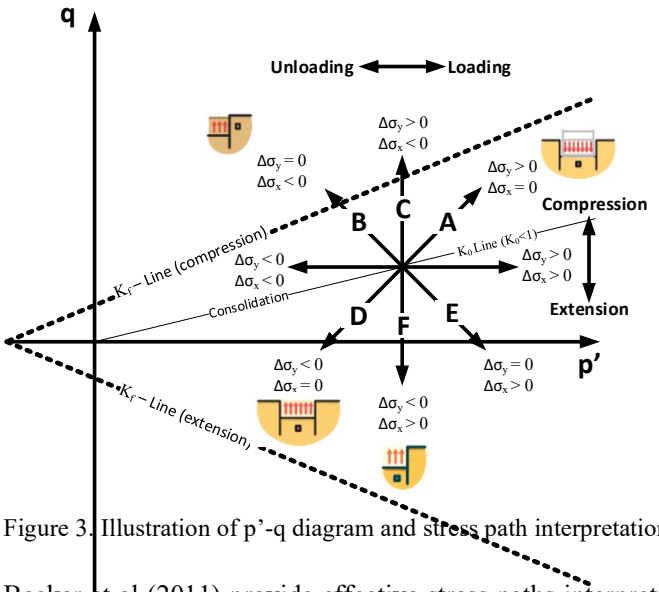


Figure 3. Illustration of p'-q diagram and stress path interpretation (Becker et al., 2011)

Becker et al (2011) provide effective stress paths interpretation and illustration of p'-q diagram in ideal condition as shown in Figure 3. According to Budhu (2011) the mean effective stress (*p'*) can be calculated using Equation (2) and deviatoric stress in axisymmetric condition can be calculated using Equation (3), while the Mohr-Coulomb failure line can also be calculated using Equation (4).

$$p' = \frac{\sigma_1' + \sigma_2' + \sigma_3'}{3} \tag{2}$$

$$q = \sqrt{\frac{(\sigma_1' - \sigma_2')^2 + (\sigma_2' - \sigma_3')^2 + (\sigma_1' - \sigma_3')^2}{2}} \tag{3}$$

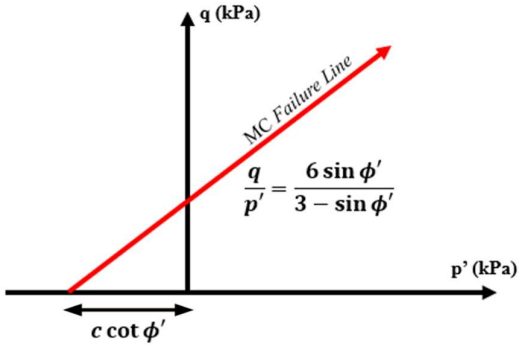


Figure 4. Mohr coulomb failure line and tension cut-off area in p'-q diagram.

$$\frac{q}{p'} = \frac{6 \sin \phi'}{3 - \sin \phi'} \tag{4}$$

## 3 RESULTS & DISCUSSION

Underconsolidating soil residual excess pore pressure was derived from the CPTu test result. Figure 5 illustrates the result of pore pressure ($U_2$) values from CPTu test and the derivation that leads to the determination of residual excess pore pressure design value. The $U_{residual}$ can be calculated using

Equation (5). According to the strain path method by Teh (1987) the pore water pressure caused by penetration of cone ($U_{cone}$) can be estimated around 5 to 7 $S_u$. In underconsolidating study case Lim et al (2016) use the $U_{cone}$ assumption of 5 $S_u$. In this analysis $U_{cone}$ will be assumed 5 $S_u$. After calculating the residual pore pressure, the design value (User defined) for initial condition of model can be determined.

$$U_{residual} = U_2 - U_{cone} - U_{static} \tag{5}$$

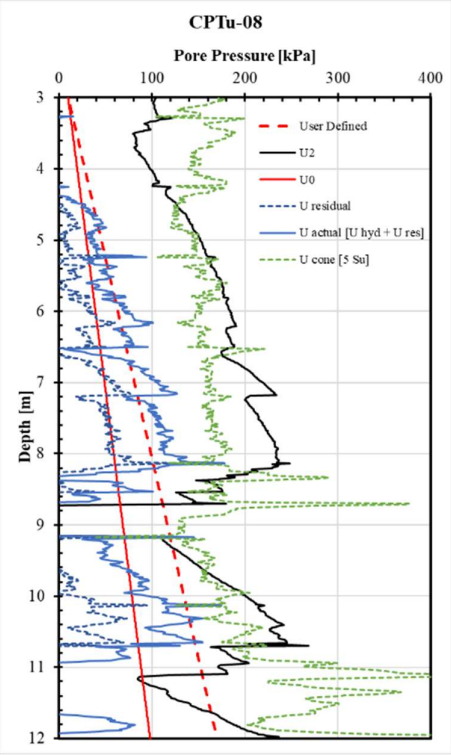


Figure 5 Measured pore pressure profile and derived values for design

Back analyses were carried out using the Mohr–Coulomb (MC) and Hardening Soil (HS) constitutive models, resulting in two sets of parameters as presented in Table 3 and Table 4. The preliminary parameters of $\gamma$, $c'$, $\phi'$, and derived from empirical correlations as described in the previous section. The model was then calibrated through back analysis to obtain compatible parameters, as summarized in Table 3. For the HS, the parameters were determined through a similar back analysis procedure, with additional calibration of the $E'_{50}$ parameter.

Table 3. The input parameters of MC soil model after back analyses

| Depth m | | | Description | $N_{spt}$ or $q_c$ | $\gamma_t$ | $E'$ | $\phi'$ | $c'$ | $\nu'_{ur}$ |
|---|---|---|---|---|---|---|---|---|---|
| | | | | | kN/m$^3$ | kPa | ° | kPa | |
| 0 | - | 3 | Fill | $q_c$ = 1000 kPa | 17 | 3900 | 30 | 13 | 0.2 |
| 3 | - | 12 | Very Soft to Soft Clay | $q_c$ = 300-600 kPa | 12 | 2600 | 26 | 5 | 0.2 |
| 12 | - | 18 | Stiff Clay | N = 20 | 16 | 46800 | 32 | 12 | 0.2 |
| 18 | - | 23 | Cemented Sand | N = 50 | 17 | 150000 | 50 | 50 | 0.2 |
| 23 | - | 40 | Stiff Clay | N = 15-20 | 17 | 39000 | 30 | 10 | 0.2 |
| 40 | - | 60 | Stiff Clay | N = 15-21 | 17 | 42900 | 30 | 11 | 0.2 |
| 60 | - | 80 | Stiff Clay | N = 15-22 | 17 | 46800 | 32 | 12 | 0.2 |

Table 4. The Input Parameters of HSM after Back Analyses

| Depth | | | Description | $E'_{50}$ | $E^{ref}_{50}$ | $E^{ref}_{oed}$ | $E^{ref}_{ur}$ |
|---|---|---|---|---|---|---|---|
| m | | | | kPa | kPa | kPa | kPa |
| 0 | - | 3 | Fill | 3000 | 7606.474 | 5324.532 | 22819.42 |
| 3 | - | 12 | Very Soft to Soft Clay | 1600 | 2210.488 | 1547.342 | 6631.464 |
| 12 | - | 18 | Stiff Clay | 37440 | 44543.69 | 31180.58 | 133631.1 |
| 18 | - | 23 | Cemented Sand | 50000 | 58328.73 | 40830.11 | 174986.2 |
| 23 | - | 40 | Stiff Clay | 31200 | 27556.97 | 19289.88 | 82670.9 |
| 40 | - | 60 | Stiff Clay | 34320 | 19579.04 | 13705.33 | 58737.11 |
| 60 | - | 80 | Stiff Clay | 37440 | 16747.95 | 11723.56 | 50243.85 |

*Note: m=1; $p_{ref}$ = 100 kPa; Rf = 0.9

Figure 6 shows the deflection of tie-back wall system and the settlement that occurs behind the wall using HS model. The deflection around 160 mm from the inclinometer reading can be considered as large deformation as the wall deflection to excavation depth ratio reaches 3% ($\delta_{hmax}$/H).

The numerical model shows that the deflection is relatively close to inclinometer data as shown in Figure 6. Under hydrostatic conditions the deformation is smaller, indicating that residual pore excess pressure induces a larger deformation towards the retaining wall in underconsolidating condition. The maximum deflection of hydrostatic condition is around 100 mm while in underconsolidating condition, wall deflection can reach up to 165 mm. Result from the settlement behind the wall also exhibited a consistent trend showing correlated value with wall deflection.

The result of numerical modelling implied the importance of modelling residual excess pore water pressure due to the underconsolidating condition, especially in cases of excavating in recently reclaimed area.

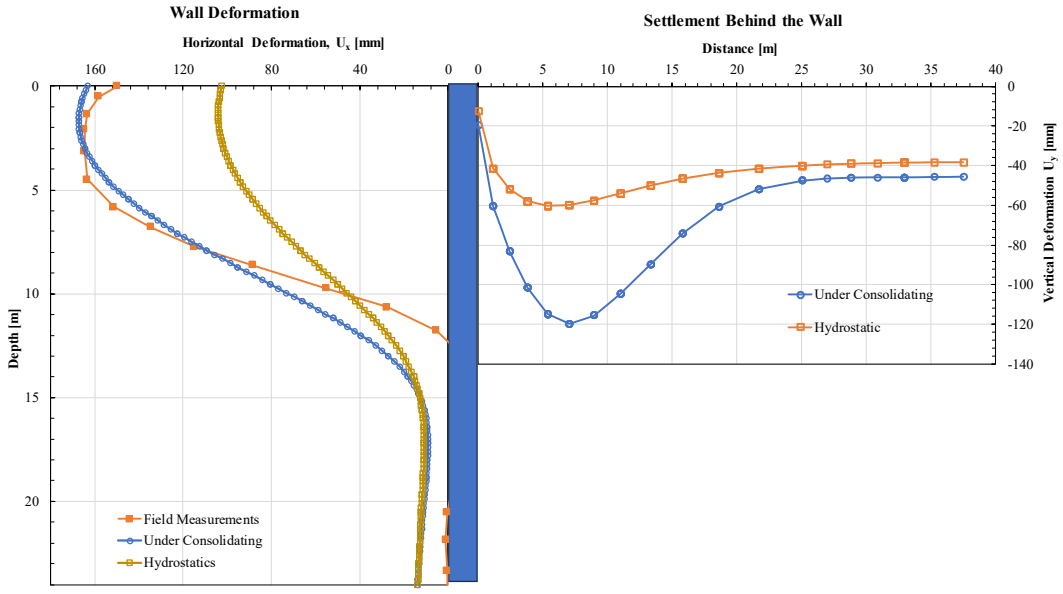


Figure 6. Wall Deflection and Settlement Behind the Wall

Figure 2 shows the selected stress points for effective stress path analysis. Eight stress points were chosen, namely A, B, C and D behind the square piles, E, F and G behind the CCSP wall and point H near the surface of the bottom of the final excavation depth. The results were plotted in *p'-q* diagram according to Budhu (2011). The effective stress path analysis was conducted for both MC

and HS model. Normally consolidated model and underconsolidating model were also plotted in the same graph to compare the stress behavior of the soil. In general, when comparing the $p'$ and $q$ values obtained from the Hardening Soil model and the Mohr-Coulomb model, the stress path of the HS model tends to move diagonally, whereas that of the MC model follows a nearly vertical linear trend. This difference arises from the constitutive behavior of each model, the MC model exhibits a linear stress–strain relationship, while the HS model follows a hyperbolic stress–strain relationship, resulting in a diagonally oriented stress path.

Figure 7 shows that at point A, the soil at underconsolidating (UC) condition moves closer to the failure line compared to normally consolidated (NC) condition, indicating an increase in the deviation between principal stress value ($\sigma_1$, $\sigma_3$) due to increase of lateral stress. Point E shows that the effective stress path is heading downward reflecting an unloading behavior in which the deviation between principal stress is decreasing and the stress state becomes more stabilized.

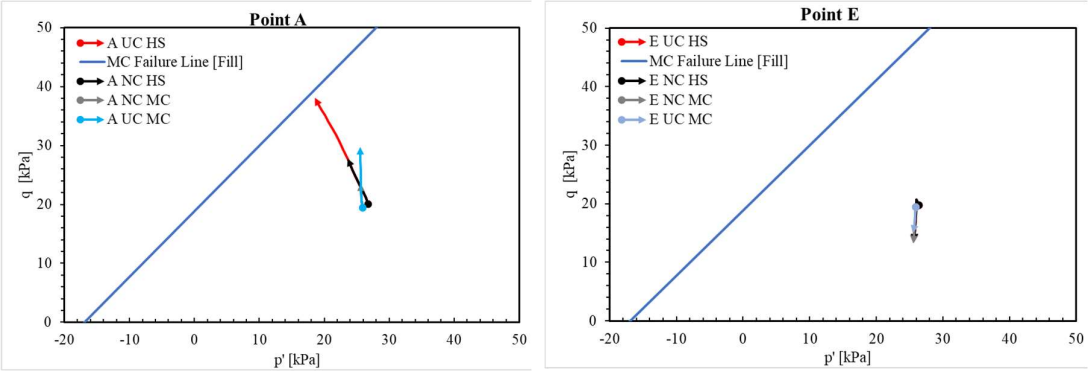


(a) (b)

Figure 7. *p'-q* diagram: (a) Point A and (b) Point E

Figure 8 presents the results of effective stress path within underconsolidating soft clay layer. Point B and F at the same depth both agree that due to the underconsolidating condition, the mean effective stresses from initial condition shift to lower values and moved closer towards failure line. This observation indicates that underconsolidating soil tends to exhibit reduced mean effective stress, which corresponds to a lower shear strength of the soil.

It is also evident that Point B exhibits a higher deviatoric stress than Point F, even though both are located at the same depth. This difference can be attributed to the position of Point F, which lies between the corrugated concrete sheet pile (CCSP) wall and the tie-back pile. The proximity of these structural elements increases the confining pressure around Point F, leading to a lower deviatoric stress. In contrast, Point B experiences less confinement, resulting in a higher deviatoric stress.

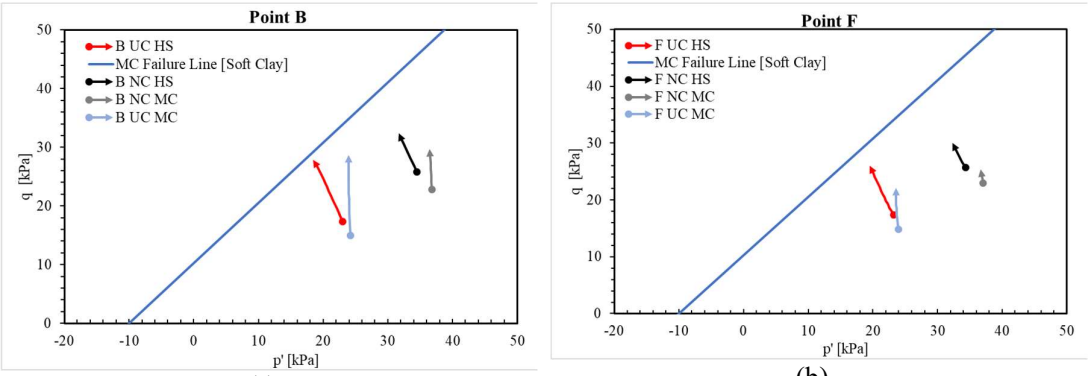


(a) (b)

Figure 8. p'-q diagram: (a) Point B and (b) Point F

Figure 9 shows the results of point C and G, which exhibit similar trend to point A. Underconsolidating condition results in the direction of stress path that is moving closer toward failure line indicating that the deviation between principal stress due to the removal of soil in excavation still has an influence of increasing deviatoric stress even at -14 m depth.

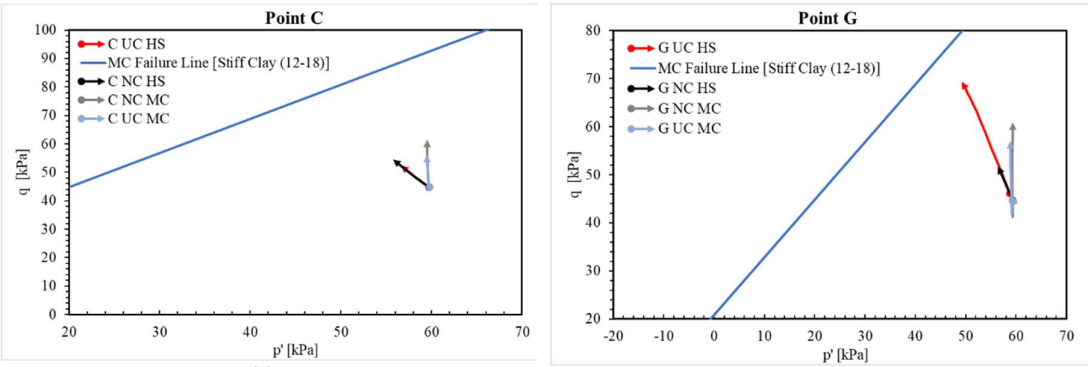


(a) (b)

Figure 9. p'-q diagram: (a) Point C and (b) Point G

Figure 10a shows the results of point D located at the bottom of square piles. The results show that the increase of deviatoric stress at this depth is relatively minor, indicating that the influence of excavation have diminished at -24 m depth. Figure 10b shows the result of point H where due to the UC condition the initial mean effective stresses shift to a lower value and move closer toward failure line. Point H results also show the behavior of unloading, as shown by the stress path downward trend from the initial state. Subsequently, the stress path rebounds upward due to the reversal of principal direction ($\sigma_1 < \sigma_3$), indicating that the lateral stress is increasing while vertical stress decreases.

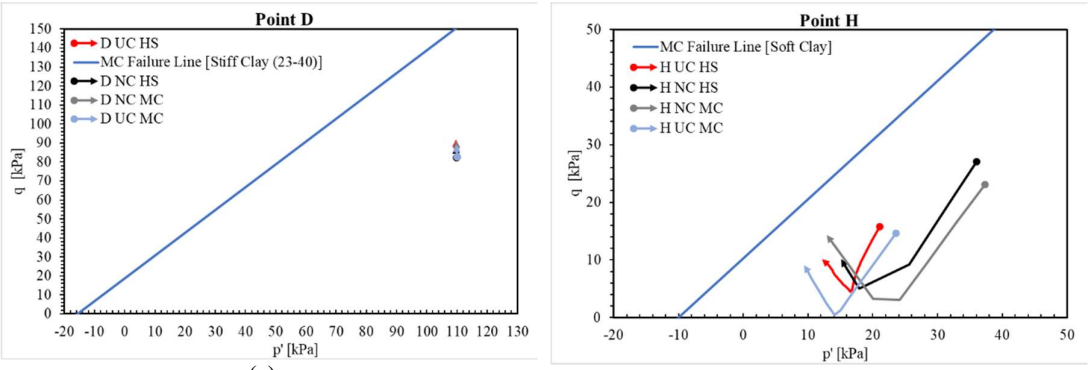


(a) (b)

Figure 10. p'-q diagram: (a) Point D and (b) Point H

### 3.1 Parametric Study

Besides the back analysis, parametric study was also carried out to understand the effect of excess pore pressure by determining a series of degree of consolidation parameters to the soil layer. In this analysis, fill layer was deactivated at initial condition. Next at the loading stage fill layer will be activated to simulate surcharge loading of soft clay layer due to the land reclamation. The loading simulation will cause the excess pore pressure to build up in soft clay layer. To simulate different consolidation stages, consolidation with varying degree of consolidation values (10%, 25%, 50%, 75% and 90%) were applied in Phase 2 to simulate the pore pressure dissipation in the soft clay layer. Prior to the structural installation and excavation process, the model displacements were reset to zero to ensure that only deformations due to excavation stages were captured. Table 5 lists the procedure for parametric study of degree of consolidation.

Table 5. Modelled phase for parametric study

| Phase | Staged Construction | Calculation Type | Pore Pressure |
|---|---|---|---|
| Initial Phase | Initial | $K_0$ Procedure | Phreatic |
| Phase 1 | Loading | Plastic | Phreatic |
| Phase 2 | Degree of Consolidation | Consolidation | Phreatic |
| Phase 3 | Structural Installation | Plastic | Previous Phase |
| Phase 4 | Excavation to -5.25 m | Plastic | Previous Phase |

The results of parametric study are shown in Figure 11. It can be seen that with the increase of excess pore pressure (lower degree of consolidation), the wall deflection will also increase. To achieve lower deformation, the consolidation process needs to be left longer to attain higher degree of consolidation. The results further stress the importance of considering excess pore pressure in the case of excavation in underconsolidating soil.

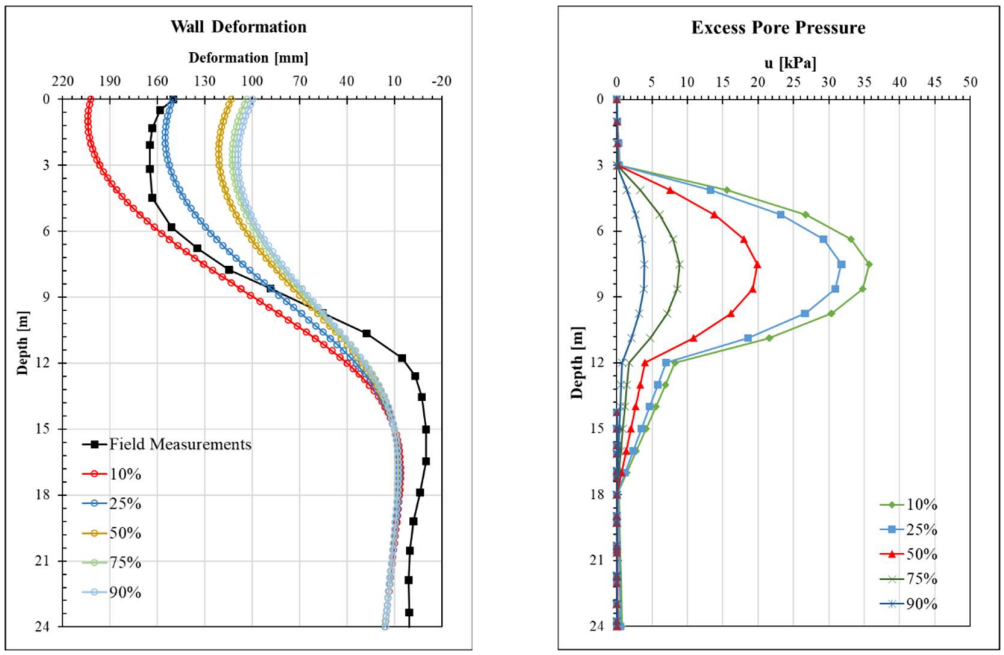


(a) (b)

Figure 11. Parametric study results: (a) wall deflection and (b) excess pore pressure in soil layer. Note: The % values in the legends refer to degree of consolidation

## 4 CONCLUSIONS

Back analyses calibrated with inclinometer data confirmed the reliability of the numerical model. The study demonstrated that under underconsolidating conditions, residual excess pore water pressure caused a maximum wall deflection of 165 mm and settlement of 120 mm behind the wall, compared to only 100 mm deflection and 60 mm settlement under fully dissipated (hydrostatic) conditions.

Stress path analysis revealed that excess pore pressure drives the stress state closer to the failure line, with effective stress decreasing and deviatoric stress increasing. At the excavation base, stress paths also revealed unloading followed by stress reversal due to changes in principal stress directions. Comparison of constitutive models indicated that the Hardening Soil (HS) model provided more realistic stress path trajectories, capturing diagonal movement due to hyperbolic stress–strain behavior, while the Mohr-Coulomb model simplified stress paths into linear, perpendicular movements. This reinforced the advantage of using HS model for evaluating complex soil behavior in excavation scenarios.

The parametric study showed a clear trend that higher degree of consolidation reduces wall deformation, showing the benefits of extending consolidation time in reducing wall deflection.

Overall, this study highlights the necessity of considering underconsolidating soil conditions and residual pore pressures in deep excavation design, particularly in reclamation areas such as North Jakarta.

## DISCLAIMER

The authors declare no conflict of interest.

## AVAILABILITY OF DATA AND MATERIALS

Some or all data, models that support the findings of this study are available from the corresponding author upon reasonable request.

## REFERENCES

Becker, P., Gebreselassie, B. & Kempfert, H.-G., 2011. Spatial effects on excavations in deep soft lacustrine clay, in *Geotechnical Aspects of Underground Construction in Soft Ground*, ed. Giulia Viggiani. Boca Raton: CRC Press, pp. 585-592. https://doi.org/10.1201/b12748-77

Budhu, M., 2011. *Soil mechanics and foundations* (3rd edition). Hoboken, NJ: John Wiley & Sons.

Calvello, M., 2004. Selecting parameters to optimize in model calibration by inverse analysis, *Computers and Geotechnics*, 31(5), pp. 410-424. https://doi.org/10.1016/j.compgeo.2004.03.002

Lambe, W. T. & Whitman, V. R., 1962. *Soil mechanics*. New York: John Wiley & Sons.

Lim, A., Anggoro, B. & Rahardjo, P., 2016. Performance and modelling of unbraced shallow excavation in under-consolidation Jakarta soft clay. *Proceeding of Soft Soil*, pp. 26-29.

Lim, A. and Ou, C.-Y., 2017. Stress paths in deep excavations under undrained conditions and its influence on deformation analysis. *Tunnelling and Underground Space Technology*, 63, pp. 118-132. doi:10.1016/j.tust.2016.12.006.

Look, B.,2007. *Handbook of geotechnical investigation and design tables*. London: Taylor & Francis.

Ou, C.-Y., 2021. *Fundamentals of deep excavations*. Boca Raton: CRC Press.

Rahardjo, P. P., Anggoro, B. W., Yakin, Y. A., & Darmawan, H., 2008. Determination of degree of consolidation of reclaimed site on deep soft Mahakam deltaic soils using CPTu. *Proceeding of the 4th International Symposium on Deformation Characteristics*.

Schanz, T., Vermeer, P. A., & Bonnier, P. G., 1999. The hardening soil model: Formulation and verification. *Proceeding of Beyond 2000 in Computational Geotechnics*, pp. 281–296.

Standards Australia, 2002. *AS 4678–2002: Earth-retaining structures*. Sydney: Standards Australia.

Setionegoro, N., 2013. *Study for site characterization of under-consolidating soft clay*. Master's Thesis, Parahyangan Catholic University.

Teh, C. I., 1987. *An analytical study of the cone penetration test*. Doctoral thesis, University of Oxford.

- This page is intentionally left blank -